ELSEVIER

Journal of Power Sources 89 (2000) 1–6

JOURNAL OF POWER SOURCES

www.elsevier.com/locate/jpowsour

Effects of temperature and partial pressure of CO_2/O_2 on corrosion behaviour of stainless-steel in molten Li/Na carbonate salt

Tae-Hoon Lim *, Eung Rim Hwang, Heung Yong Ha, Suk Woo Nam, In-Hwan Oh, Seong-Ahn Hong

Battery and Fuel Cell Research Center, Korea Institute of Science and Technology, 39-1 Hawolgok-dong, Sungbuk-gu, Seoul, 136-791, South Korea

Received 2 September 1999; accepted 7 December 1999

Abstract

The corrosion tests with AISI-type 316L and 310S stainless steels are carried out to understand the abnormal corrosion behaviour observed in a molten 52 m/o Li_2CO_3–48 m/o Na_2CO_3 salt in the temperature range of 520°C to 580°C, particularly in the presence of CO_2 and O_2. Two experimental methods, namely, an out-of-cell test and an electrochemical method, were employed to analyze the corrosion behaviour with varying gas composition as well as temperature. The samples tested in the temperature range of 520°C to 580°C suffer more corrosion attack than those tested in the temperature range of 600°C to 650°C. Optical microscope analysis of samples from out-of-cell tests for 100 h show that the surfaces of the samples, regardless of the type of stainless-steel, were corroded severely by pitting when the temperature is below 580°C. Samples tested above 600°C, however, do not suffer significant corrosion attack. This is also confirmed by potentiodynamic results. The polarization curves of 316L stainless-steel samples measured above 600°C exhibit the typical active–passive behaviour, but the passive region disappears when the temperature is below 580°C. This is attributed to the formation of a porous $LiFe_5O_8$ passive film. By contrast, the formation of a $LiFeO_2$ passive film, dense enough to provide protection, is observed with increasing temperature over 600°C. It is also found that the partial pressure of CO_2 affects markedly the corrosion rate, but the partial pressure of O_2 does not.

Keywords: Molten carbonate fuel cell; Stainless-steel; Li/Na carbonate; Corrosion; Passive film

1. Introduction

A fuel cell is an energy-conversion device which generates electricity directly through an electrochemical reaction between, for example, hydrogen and oxygen [1]. This makes fuel cell free from the Carnot cycle limitation, which, in turn, enables the fuel cell to have high efficiency in electricity generation and less production of pollutants. The molten carbonate fuel cell (MCFC) system possesses several other advantages due to its high operation temperature of 650°C. These advantages include high quality of waste heat, fuel flexibility and internal reforming. On the other hand, a high operation temperature combined with the presence of very corrosive Li/K molten carbonate requires expensive materials to withstand the harsh conditions. This has delayed the commercialization of MCFC technology. It is generally accepted that a lifetime of at least 40 000 h is required to be competitive in the market [2]. So far, no MCFC system, regardless of its size, has been successful in achieving the lifetime target. Loss and redistribution of electrolyte, corrosion of metallic components, morphology changes of porous components, phase transformation, and short-circuiting by NiO dissolution are responsible for the lifetime limitation [3]. Among many approaches to solve the lifetime issues, replacement of electrolyte composition from Li/K carbonate to Li/Na carbonate is considered to be an option [4–6].

The Li/Na electrolyte (52 m/o Li_2CO_3–48 m/o Na_2CO_3) for the MCFC has a few advantages over conventional Li/K (62 m/o Li_2CO_3–38 m/o K_2CO_3), especially in the areas of ionic conductivity, electrolyte inventory management, and NiO dissolution. Nevertheless, it has been seldom used as an electrolyte for MCFCs because of the low oxygen solubility in Li/Na carbonate mixture. The performance of a MCFC with Li/Na electrolyte is

* Corresponding author. Tel.: +82-2-958-5273; fax: +82-2-958-5199.
E-mail address: thlim@kistmail.kist.re.kr (T.-H. Lim).

0378-7753/00/$ - see front matter
PII: S0378-7753(00)00376-1

usually lower than that with Li/K at atmospheric pressure. The polarization of the former cell caused by low oxygen solubility decreases and, eventually, becomes less than that of the latter cells with increasing operation pressure. NiO dissolution is the most crucial determinant of life. In this respect, therefore, Li/Na electrolyte is expected to replace, or has already begun to replace, Li/K electrolyte.

Another problem associated with using Li/Na as electrolyte is the unusual and excessive corrosion phenomenon on the separator which is observed in the cathode gas atmosphere containing air and CO_2 at the particular temperature range of 520°C to 600°C [7,8]. This corrosion does not exist at over 600°C. It is a well-known fact that AISI 316L or 310S, high chromium-content, stainless-steel is the most widely used material for the separator of MCFCs as it can provide sufficient corrosion resistance against Li/K electrolyte under normal MCFC operating conditions. These high-chromium-content stainless-steels are able to form protective passive films which consist of two layers, i.e., an external $LiFeO_2$ layer and an internal chromium-rich layer. This duplex passive film can prevent further corrosion by suppressing the outward diffusion of cations such as Fe^{+2}. On the other hand, the low-chromium-content alloy (for example, only 2 to 2.5 wt.% Cr) is corroded very severely when exposed to a Li/K carbonate melt because it lacks ability to form a protective chromium-rich oxide layer. Non-protective porous oxide films of Fe_3O_4 and $LiFe_5O_8$ are produced instead [9]. Although the corrosion of the separator in a Li/Na carbonate melt behaves differently from that in a Li/K carbonate melt, there is little information on this. Taking into consideration the decisive effect of the pretreatment procedure on MCFC performance, in which the temperature is raised from ambient to 650°C, the gas composition should be adjusted properly in relation with the temperature to avoid corrosion when Li/Na electrolyte is used. Otherwise, excessive corrosion will take place at the cathode side between 520°C and 600°C. Thus, in this paper, the corrosion behaviour has been investigated with emphasis on analysis of the corrosion product as well as on the effect of temperature and gas composition.

2. Experimental

All the samples made with AISI 316L or 310S stainless-steel were homogenized prior to the corrosion test by heat treatment at 1200°C for 4 h in vacuum, followed by quenching with ice water. After cutting into a square ($20 \times 20 \times 1$ mm), each specimen was polished to have mirror-like surface.

The out-of-cell test was carried out to obtain an overall view of the corrosion process in the presence of 52 m/o Li_2CO_3–48 m/o Na_2CO_3 by analyzing corrosion morphology and product with optical microscope and X-ray diffraction (XRD). To simulate the corrosion environment of the wet-seal area of the MCFC, which is the most susceptible region to corrosion of the separator, a specimen was inserted between electrolyte/matrix green sheets at ambient temperature, then heated to a desired temperature in argon atmosphere. Upon arriving at a desired temperature, the gas composition was switched to either the standard cathode condition (67% CO_2–33% O_2) or Ar–O_2/Ar–CO_2. The partial pressures of O_2 or CO_2 were varied from 0 to 0.6 atm, respectively. After staying for 100 h at a given experimental condition, the specimen was removed from the furnace. The corrosion rate was determined by weight difference of the specimen between before the experiment and after peeling off the corrosion product. To dissolve off the corrosion product, the specimen was boiled for 12 h in 18% NaOH–3% $KMnO_4$ solution followed by 3 h in 10% $(NH_4)_2HC_6H_5O_7$ solution [10].

Electrochemical experiments were conducted in a so-called pot cell [11]. The working electrode was made of stainless-steel which was spot-welded to a gold wire (99.9% pure, 0.5 mm in diameter). A gold foil ($25 \times 80 \times 0.5$ mm) was used as the counter electrode. The reference electrode consisted of a gold wire and double alumina tubes. The external tube had a small hole of 3 μm in diameter at the bottom to form a salt bridge. The gas composition fed to the reference electrode was 67% CO_2–33% O_2. The gold wire in the tube was in contact with the 52 m/o Li_2CO_3–48 m/o Na_2CO_3 melt through the salt bridge. The potentiodynamic curves of the samples were recorded from −1400 to +400 mV at a scan rate of 0.1 mV s^{-1}. Cyclic voltammograms were obtained between −1700 and +100 mV at a scan rate of 50 mV s^{-1}. All the electrochemical measurements were performed with an EG&G potentiostat/galvanostat (Model 273A).

3. Results and discussion

3.1. Effect of temperature in standard cathode gas atmosphere (67% CO2–33% O2)

The effect of temperature on the weight loss of a 316L or a 310S sample during a 100-h out-of-cell test in the temperature range of 520°C to 650°C under cathode gas atmosphere is shown in Fig. 1. Severe corrosion attack on both stainless-steels is observed at temperatures below 580°C. After reaching a maximum value at near 580°C, the weight loss decreases rapidly as the temperature approaches 620°C. The weight loss then increases again due to a faster corrosion reaction with increasing temperature. Although 316L stainless-steel shows higher susceptibility to corrosion in general, the shapes and trends of weight

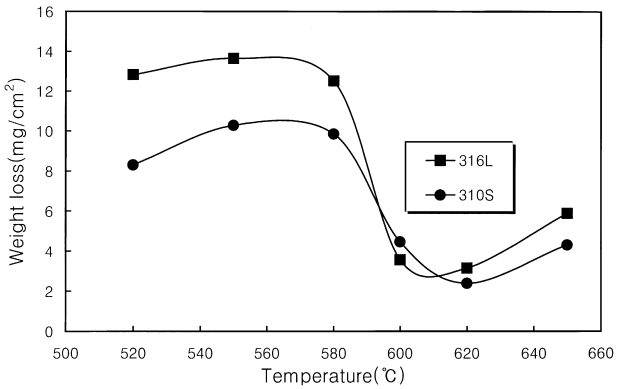

Fig. 1. Effect of temperature on corrosion. (electrolyte: 52 m/o Li_2CO_3–48 m/o Na_2CO_3, cathode atmosphere).

loss vs. temperature for both stainless-steels are similar. This result indicates that the corrosion on both samples in the Li/Na carbonate melt may proceed via the same mechanism.

From the difference between corrosion products formed below 580°C and above 620°C, however, it can be deduced that there is a change in the corrosion mechanism around 600°C. A porous red-brown scale was observed on the surface of the stainless-steels below 580°C, whereas a dense black scale was observed above 600°C. The XRD analyses of corrosion products of 316L at 580°C and 650°C are given in Fig. 2. Large differences are found in the major component of corrosion product, i.e., $LiFe_5O_8$ at 580°C vs. $LiFeO_2$ at 650°C, and in the degree of crystallization of the corrosion product. Minute but continuous pertubation of the of base line of the XRD pattern in Fig. 2(b) imply a less crystalline or porous nature of corrosion product formed at 580°C. The change of corrosion product from $LiFeO_2$ to $LiFe_5O_8$ with decreasing temperature observed in this study is in good agreement with the thermodynamic calculations of Matsumoto et al. [12]. According to their findings, $LiFeO_2$, which is the more stable phase at 650°C, will be transformed into $LiFe_5O_8$ as temperature decreases to 550°C in the standard cathode gas atmosphere of the MCFC. Considering the fact that the composition of corrosion product in the Li/Na carbonate melt is almost identical with that in the Li/K carbonate melt, the morphology of the corrosion product on the surface of the stainless-steel appears to be an important determinant of the corrosion rate. The metal oxide layer formed on the surface of austenitic stainless steels in a Li/K carbonate melt is generally assumed to be insoluble and dense so that the oxide layer could retard further corrosion attack [13]. As explained above, the metal oxide layer formed on the surface of stainless steels in a Li/Na carbonate melt below 580°C is porous $LiFe_5O_8$, which is not able to provide the protection against further corrosion attack. This eventually causes abnormal and excessive corrosion which does not exist in a Li/K carbonate melt under the same conditions. This unique corrosion phenomenon will disappear due to the formation of dense double-layered corrosion scale consisting of an external $LiFeO_2$ layer and an internal $LiCrO_2$ layer when the temperature rises above 600°C. It still requires more investigation, however, to determine what makes the corrosion in a Li/Na carbonate melt behave differently from that in a Li/K carbonate melt.

The surface morphology of de-scaled 316L stainless-steel after an out-of-cell test for 100 h in the temperature range of 520°C to 650°C was examined by means of an optical microscope. Results are shown in Fig. 3. Up to 580°C, successive corrosion did take place at the surface of stainless-steel just beneath the corrosion scale. Severe pitting corrosion as well as intergranular corrosion (IGC) caused by sensitization can be easily identified. Pitting corrosion is often observed when the passive film fails to act as a barrier to the diffusion of ions involved in the corrosion [14]. In this case, pitting corrosion is attributed to the local environment developed by the concentration profile of the gaseous species through porous passive film. By constrast, as temperature increases above 600°C, only traces from IGC attack are visible. These observations are comparable with the findings in Figs. 1 and 2.

The anodic polarization curve generated potentiodynamically for 316L stainless-steel in a Li/Na carbonate melt in the cathode gas atmosphere is shown in Fig. 4. When measured at 550°C and 580°C, the passive regions totally vanish. The passive region begins to appear at 620°C and fully develops at 650°C with the typical active–passive corrosion behaviour. Further evidence is given in Fig. 4 for the transition of the nature of passive film on the surface of the stainless-steels in a Li/Na carbonate melt from non-protective below 580°C to protective above 600°C. The result of the experiment with a Li/K carbonate in the same condition always shows the active–passive transition behaviour regardless of the temperature range [15].

In order to identify the reactions associated with the formation of the passive film on the stainless-steel in a Li/Na carbonate melt, cyclic voltammetric tests of the 316L stainless-steel were performed in the temperature

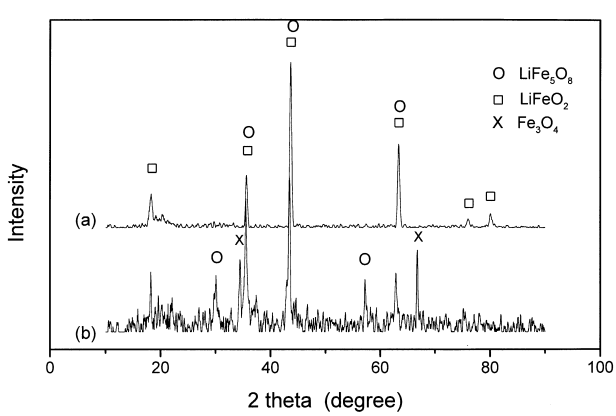

Fig. 2. XRD pattern of 316L stainless-steel corroded in Li/Na carbonate melt for 100 h under cathode gas atmosphere at (a) 650°C and (b) 580°C.

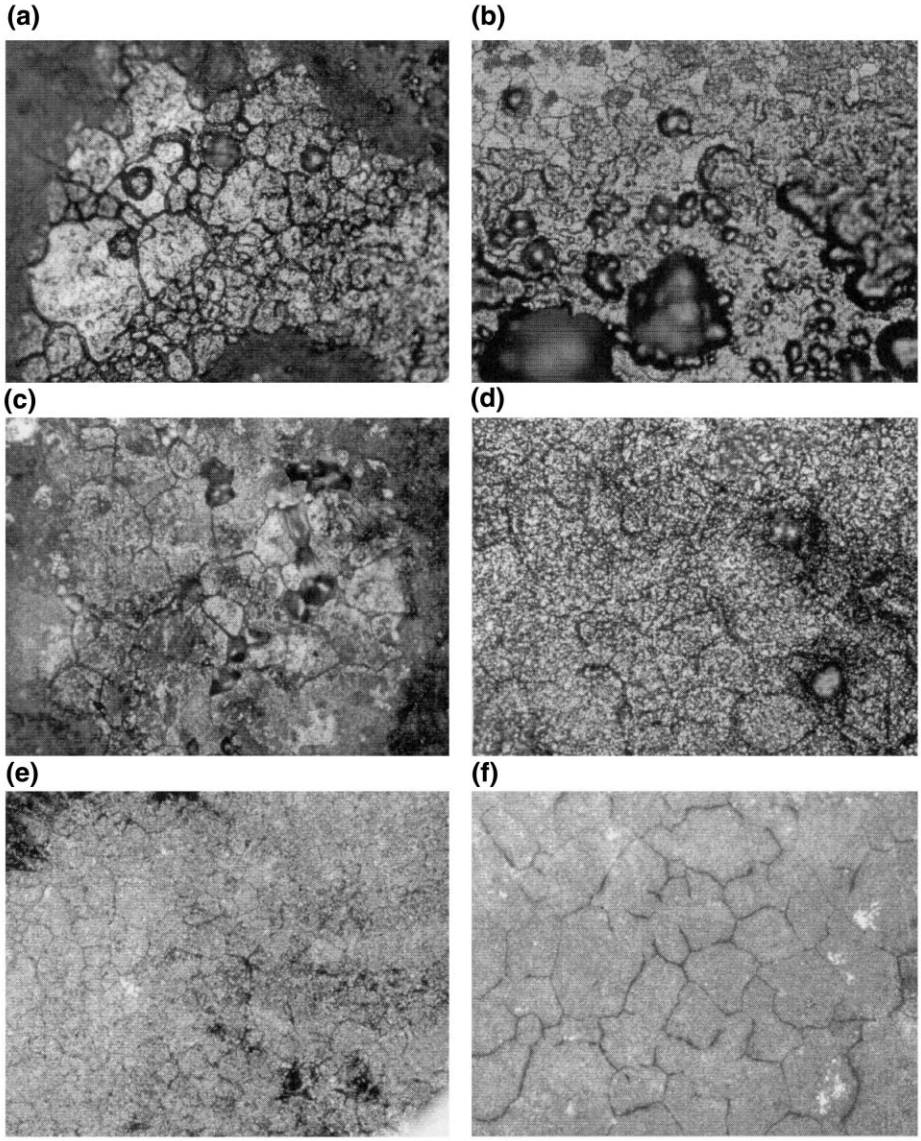

Fig. 3. Surface morphology of descaled-316L stainless-steels corroded in Li/Na carbonate melt under cathode gas atmosphere at (a) 520°C, (b) 550°C, (c) 580°C, (d) 600°C, (e) 620°C, and (f) 650°C (×500).

range of 580°C to 650°C. The results obtained at 580°C and 650°C, are illustrated in Fig. 5. In the range −1.4 to −0.5 V, two oxidation peaks and the corresponding reduction peaks are observed for both temperatures. According to Vossen et al. [16], the first peak and the second peak can be ascribed to the oxidation of iron to FeO or $LiFeO_2$ and to α-$LiFeO_2$ or α-$LiFe_5O_8$, respectively. Even if these peak assignments cannot be guaranteed for our data since they were acquired under the anodic gas condition in Li/K carbonate at 650°C, they provide several key insights into the film formation on the 316L stainless-steel surface. The first peak at 650°C is shifted to a more positive potential than that at 580°C, which explains slow kinetics via dense film formation at 650°C. Surprisingly, what should be noticed in this graph is the increase of current density of the second peak at 580°C compared with that at 650°C. This result means that the corrosion at 580°C, which produces α-$LiFe_5O_8$, is much larger than that at 650°C. A further interesting observation is the appearance of the third peak at 580°C, although not clearly visible due to the maximum current limitation (1A) of the potentiostat used in the experiment, with increasing the potential beyond −0.5 V. The oxidation of Cr at the scale/stainless-steel interface due to insufficient passivity of α-$LiFe_5O_8$ is thought to be responsible for the third peak. By contrast, there is no additional peak at 650°C. The small current density of the second peak combined with the absence of the third peak verifies that the passivity of α-$LiFeO_2$ film formed at 650°C is sufficient to suppress the diffusion of carbonate ions and metal cations.

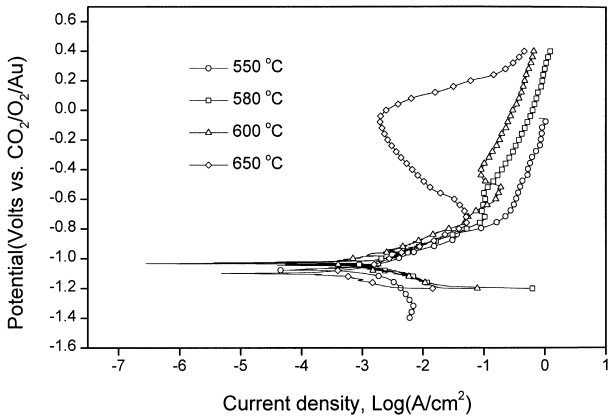

Fig. 4. Anodic polarization behaviour of 316L stainless-steel in Li/Na carbonate melt at various temperatures.

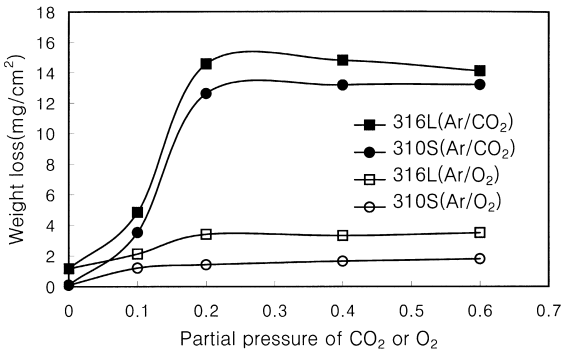

Fig. 6. Effect of partial pressures of CO_2 and O_2 on corrosion rate of 316L and 310S stainless-steels (Li/Na carbonate melt, 580°C, 100 h).

3.2. Effect of partial pressure of CO2 and O2

Because the abnormal corrosion phenomenon took place only when CO_2 and O_2 were present, the effect of partial pressures of CO_2 and O_2 was examined. The partial pressure of each gas was varied from 0 to 0.6 atm and the balance was argon. The corrosion rates measured as the weight loss of 316L and 310S stainless-steel samples after out-of-cell tests for 100 h at 580°C are presented in Fig. 6. There is no large difference in the corrosion behaviour of the two stainless-steels in either Ar–CO_2 or Ar–O_2 atmosphere, but 310S stainless-steel shows higher resistance against corrosion than 316L stainless steel throughout the whole experimental conditions. As clearly seen in Fig. 6, the corrosion rate depends mainly on the partial pressure of CO_2 but little on the partial pressure of O_2. It is also observed that the corrosion rate increases very rapidly with the increase of the partial pressure of CO_2 until it reaches plateau at a partial pressure of 0.2 atm or above where saturation of dissolved CO_2 in Li/Na electrolyte is expected. This implies participation of the dissolved CO_2 in the corrosion reaction in a Li/Na carbonate melt. The dissolved CO_2 is considered to possibly involve two corrosion mechanisms as follows: (1) As CO_2 dissolves in the Li/Na electrolyte, the electrolyte becomes more acidic. And this higher acidity makes metal oxide scale more soluble in the electrolyte, in consequence, leading to an enhanced the corrosion rate. (2) The dissolved CO_2 can play an important role, to some extent, in deciding the composition of metal oxide scale. Taking the very low solubility of the metal oxide scale in the Li/Na electrolyte into account, however, the second mechanism seems to be more feasible.

One of the major corrosion reactions of stainless-steel in a Li/Na carbonate melt can be represented by:

$$Fe + 1/2Li_2CO_3 + 3/4O_2 = LiFeO_2 + 1/2CO_2. \quad (1)$$

This suggests that high O_2 or/and low CO_2 partial pressure favours the formation of $LiFeO_2$, which is known to be a protective passive film [13]. In other words, increasing the partial pressure of CO_2 will reduce the formation of $LiFeO_2$ by an equilibrium shift in favour of the reverse reaction of Eq. (1). Based on thermodynamic data [17], $LiFe_5O_8$, the more stable phase at high CO_2 partial pres-

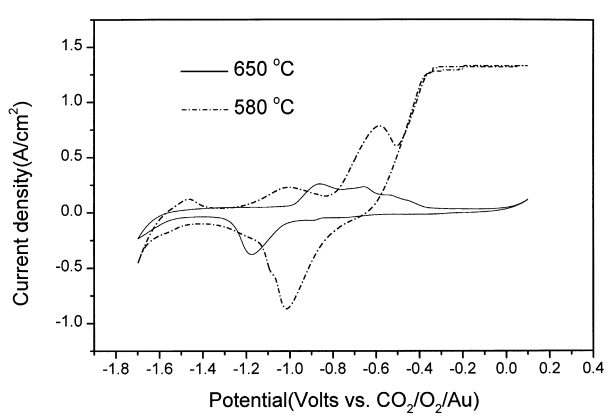

Fig. 5. Cyclic voltammograms of 316L stainless-steels in Li/Na carbonate melt under cathode gas atmosphere at 580°C and 650°C.

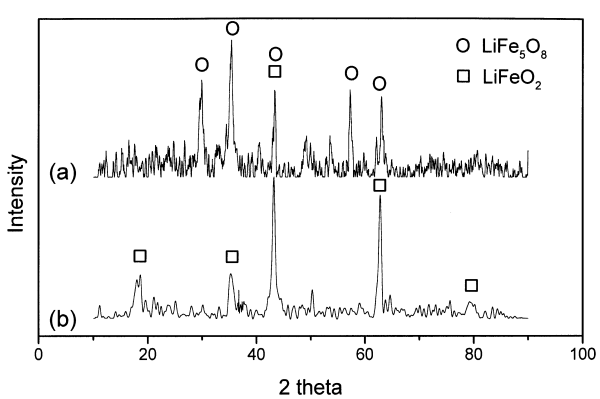

Fig. 7. XRD patterns of 316L stainless-steels corroded in Li/Na carbonate melt at 580°C for 100 h under (a) Ar–40% CO_2 and (b) Ar–40% O_2 atmosphere.

sure, is likely to be produced instead. The XRD patterns of metal oxide scales on 316L stainless-steel in Ar–40% CO_2 and Ar–40% O_2 atmosphere are given in Fig. 7. In an Ar–40% CO_2 atmosphere, $LiFe_5O_8$ is the dominant component in the metal oxide scale, and $LiFeO_2$ in Ar–40% O_2 atmosphere. Comparison of the baseline of XRD patterns also indicates that the former compound has a more porous structure than the latter. The formation of $LiFe_5O_8$ scale along with its porous morphology supports the higher susceptibility of stainless-steel to corrosion in a Li/Na carbonate melt in a CO_2-rich atmosphere.

4. Conclusions

From the present investigation on the corrosion behaviour of 316L and 310S stainless-steels in a molten Li/Na carbonate salt, the following conclusions can be drawn.

(1) Temperature has profound effect on the corrosion behaviour of 316L and 310S stainless-steels in a Li/Na carbonate melt in a cathode gas atmosphere (67% CO_2–33% O_2). Severe attack occurs mainly by pitting due to the formation of porous $LiFe_5O_8$ below 580°C. On the other hand, due to the formation of dense $LiFeO_2$, little corrosion attack other than IGC by a sensitization effect is observed above 620°C. It is believed that there is a change in corrosion mechanism around 600°C. The potentiodynamic analysis of 316L stainless-steel shows only active behaviour below 580°C, but typical active–passive behaviour at 650°C.

(2) The gas atmosphere also plays an important role in determining the corrosion behaviour of stainless-steels in a Li/Na carbonate melt. The corrosion rates of 316L and 310S stainless-steels depend significantly on the partial pressure of CO_2 but very little on the partial pressure of O_2. The suppression of protective $LiFeO_2$ formation combined with thermodynamic encouragement of non-protective $LiFe_5O_8$ formation in CO_2-rich atmosphere is considered to be responsible for this phenomenon.

References

[1] Proc. 3rd Symp., Carbonate Fuel Cell Technology, PV93-3, M.C. Williams, E.L. Parsosns, T.J. George (Eds.), The Electrochem. Soc. 1993, p. 1.
[2] S.S. Penner, in: Assessment of Research Needs for Advanced Fuel Cells, Pergamon, Oxford, 1986, p. 153.
[3] J.H. Hirschenhofer, D.B. Stauffer, R.R. Engleman, Fuel Cells A Handbook, US DOE, 1994, (Revision 3).
[4] S. Yoshioka, H. Urushibata, Denki Kagaku 64 (1996) 909.
[5] K. Yamada, T. Nishina, I. Uchida, Electrochim. Acta 40 (1995) 1927.
[6] Y. Mugikura, F. Yoshiba, Y. Izaki, T. Watanabe, K. Takahashi, S. Takashima, T. Kahara, J. Power Sources 75 (1998) 108.
[7] K. Matsumoto, A. Matsuoka, K. Nakagawa, K. Takizawa, Denki Kagaku 65 (1997) 44.
[8] K. Ota, K. Toda, N. Motohira, N. Kamiya, Accelerated corrosion of stainless steel below 923 K with the presence of molten carbonate, Abstract in MRS 1998 Fall Meetings.
[9] M. Spiegel, P. Biedenkopf, H.J. Grabke, Corros. Sci. 39 (1997) 1193.
[10] M. Sasaki, S. Ohta, N. Igata, Zairyo to Kankyo 45 (1996) 192.
[11] E.R. Hwang, J.W. Park, Y.D. Kim, S.J. Kim, S.G. Kang, J. Power Sources 69 (1997) 59.
[12] K. Matsumoto, K. Yuasa, K. Nakagawa, Denki Kagaku 67 (1999) 253.
[13] R.A. Donado, L.G. Marianowski, H.C. Maru, J.R. Selman, J. Electrochem. Soc. 131 (1984) 2535.
[14] D.A. Jones, in: Principles and Prevention of Corrosion, 2nd edn., Macmillan, New York, 1986, p. 199.
[15] K.S. Lee, K. Cho, T.H. Lim, S.-A. Hong, H. Kim, J. Power Sources, in press.
[16] J.P.T. Vossen, L. Plomp, J.H.W. de Wit, G. Rietveld, J. Electrochem. Soc. 142 (1995) 3327.
[17] S. Mitsushima, N. Kamiya, K. Ota, K. Toda, J. Electrochem. Soc. 137 (1990) 2713.